# Supporting Materials

## Electrocatalytic hydrogenation of indigo by NiMoS: energy saving and conversion improving

Zihao Liu, Xunkai Yu, Jie Li, Dong Wei, Junjun Peng, Huiyu Jiang, Huihong Liu*

**Affiliation 1**: School of Chemistry and Chemical Engineering, Hubei Key Laboratory of Biomass Fibers and Eco-dyeing & Finishing, Wuhan Textile University, No.1 Sunshine Avenue, Wuhan 430200, People's Republic of China.

**Corresponding authors:**

H. H. Liu (Email: huihongliu@126.com or huihongliu@wtu.edu.cn).

**Addresses:** No.1 Sunshine Avenue, Jiang Xia District, Wuhan, 430200, People's Republic of China.

**ORCID:** 0000-0002-2192-8698

**Figure S1. SEM & EDX (A) Carbon felt; (B) Ni/CF; (C) NiMo/CF**

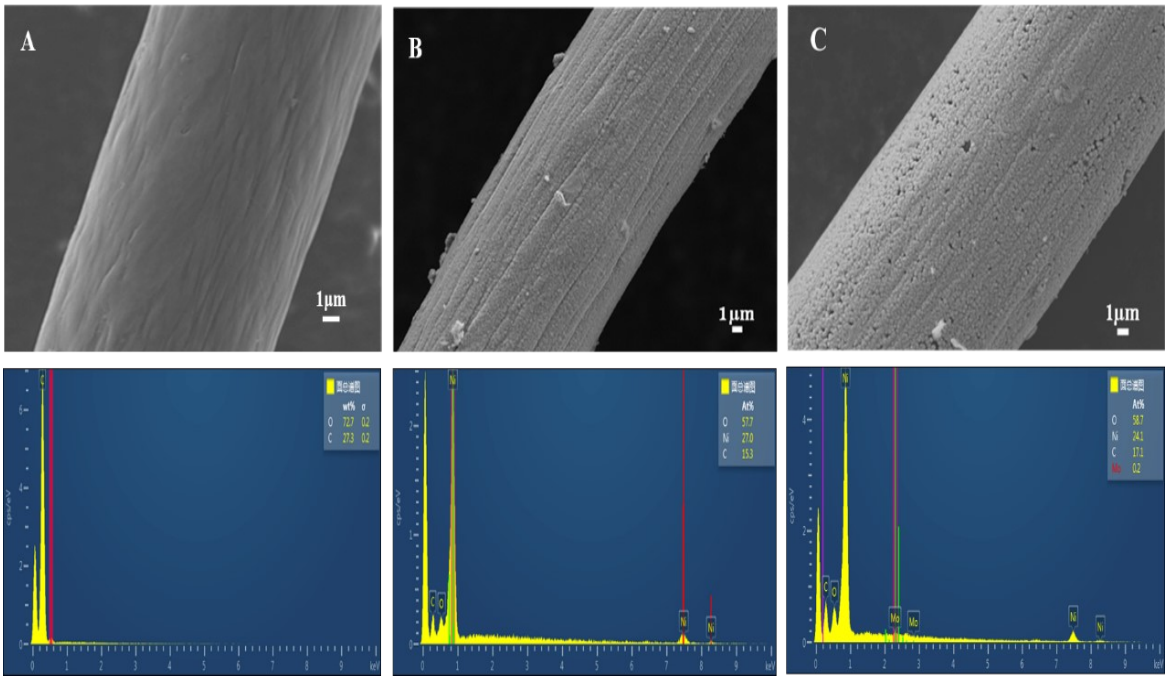

## The characterization of NiMoS300, NiMoS600, and NiMoS900

**Although** the overpotential of 96.0 mV by NiMoS600 for splitting water is fewer negative then 89.0 mV by NiMoS300, NiMoS300 is easily dislodged during the water electrolysis. As for NiMoS900, the overpotential of 280.1 mV is more negative than those of NiMoS600 and NiMoS300 (**Fig.S4**).

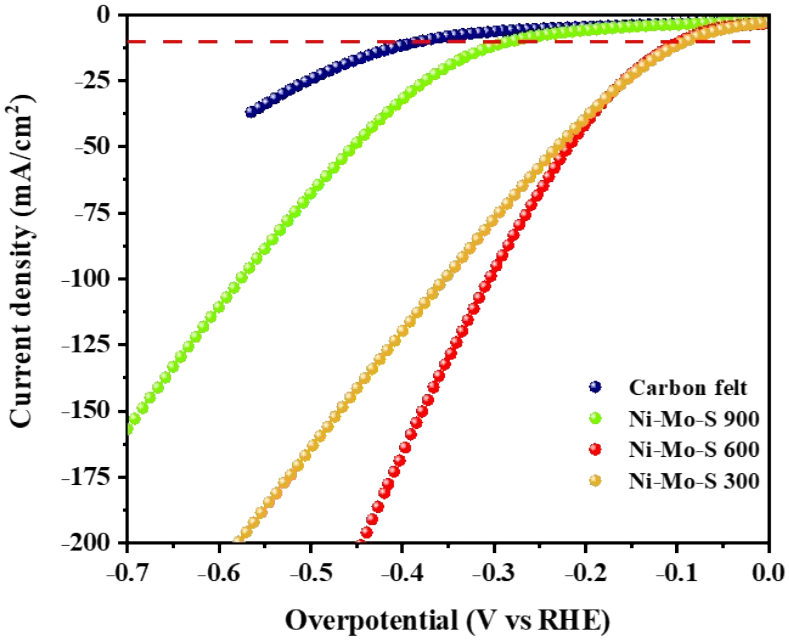


**Fig.S2**. Polarization curves of Carbon felt, NiMoS300℃/CF, NiMoS600℃/CF and NiMoS900℃/CF at scan rate of 5 mV/s in 1.0 M KOH

The electrochemically active surface area (ECSA) is an indicator of the exposed active sites on the electrode surface. In general, increasing ECSA is an effective way to improve the electrocatalytic activity of catalysts. The results showed that the highest Cdl values were obtained when the temperature was 600 °C in the same substrate (**Fig.S3A)**. The Cdl values of samples were depicted in cyclic voltammograms (**Fig.S3B).** For

example, the Cdl value of NiMoS600 (36.2 mF $cm^{-2}$) is bigger than that of NiMoS300 (35.8 mF $cm^{-2}$), NiMoS900 (31.8 mF $cm^{-2}$), indicating that NiMoS600 possesses the most activity sites comparing to the controlled electrodes.

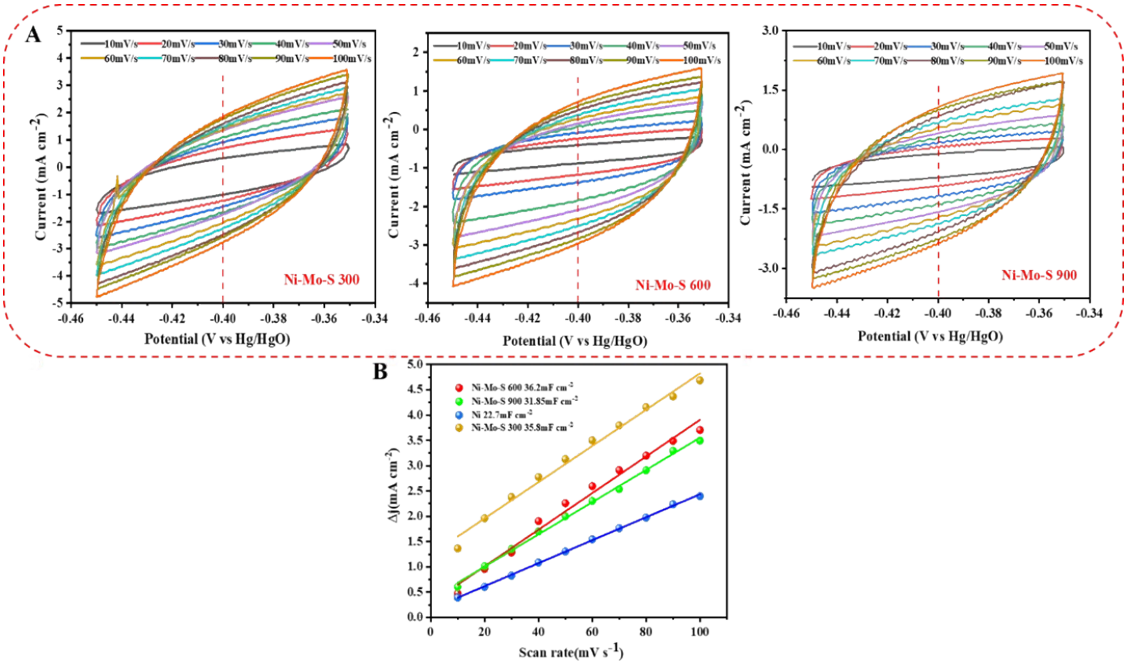


**Fig.S3**. (A)CV curves at different vulcanization temperatures (B)Plot of current density versus scan rate for CV curve fitting at different temperatures.

Electrochemical impedance spectroscopy was used to estimate the value of Rct which evaluates the electron transfer at the electrode/electrolyte interface. From (**Fig.S4**) we can see that the value of NiMoS600 (182 Ω) is lower than that of NiMoS300 (229.6Ω) and NiMoS900 (877.3Ω), indicating that the NiMoS600 can accelerate the electron transfer in water dissociation fast than that of the other electrodes as-prepared.

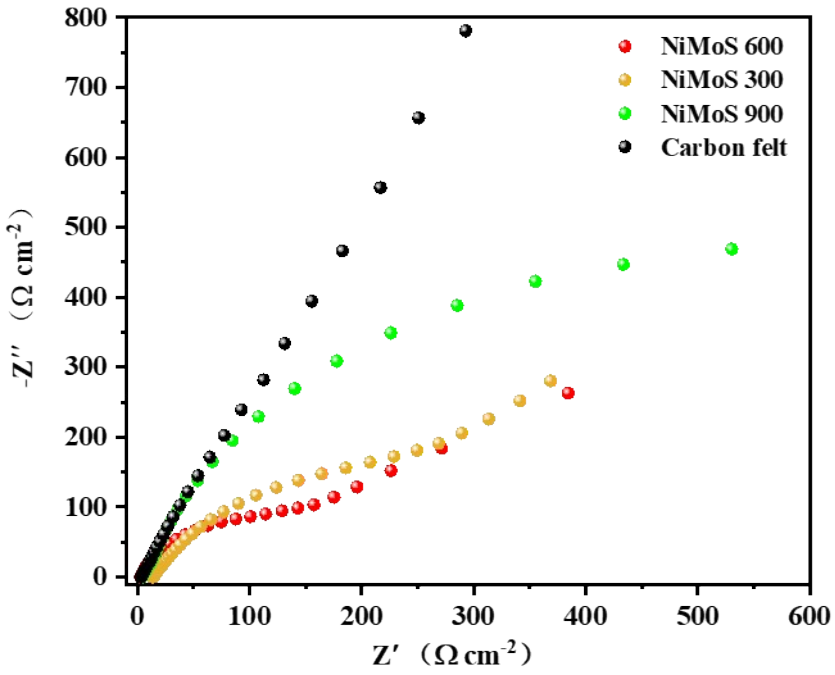


**Fig.S4**. Nyquist plots of CF, NiMoS300℃/CF, NiMoS600℃/CF and NiMoS900℃/CF in the frequency range of $10^5$ to 0.01 Hz.

The X-ray diffraction peaks of NiMoS/CF at different vulcanization temperatures are shown in **Fig.S5**. The samples at 300°C were consistent with $NiS_2$ standard pattern (PDF#88-1709). The obvious diffraction peaks occur at 27.14°, 31.43°, 31.29°, 38.75°,45.05° and 53.38° corresponding to the (111), (200), (210), (211), (220) and (311) planes of the $NiS_2$ crystal[1]. The $Ni_3S_2$ (PDF#85-1802) phase is mainly formed at temperatures of 600 and 900°C. The obvious diffraction peaks occur at 21.77°, 31.10°, 37.81°, 44.30°,49.70° and 50.01° corresponding to the (101), (110), (003), (202), (113) and (122) planes of the $Ni_3S_2$ crystal. Unlike the reaction occurring at 600 °C, the conversion of the film into $MoS_2$ (PDF#77-0341) did not take place at 900 °C most likely by virtue of excessive temperature.

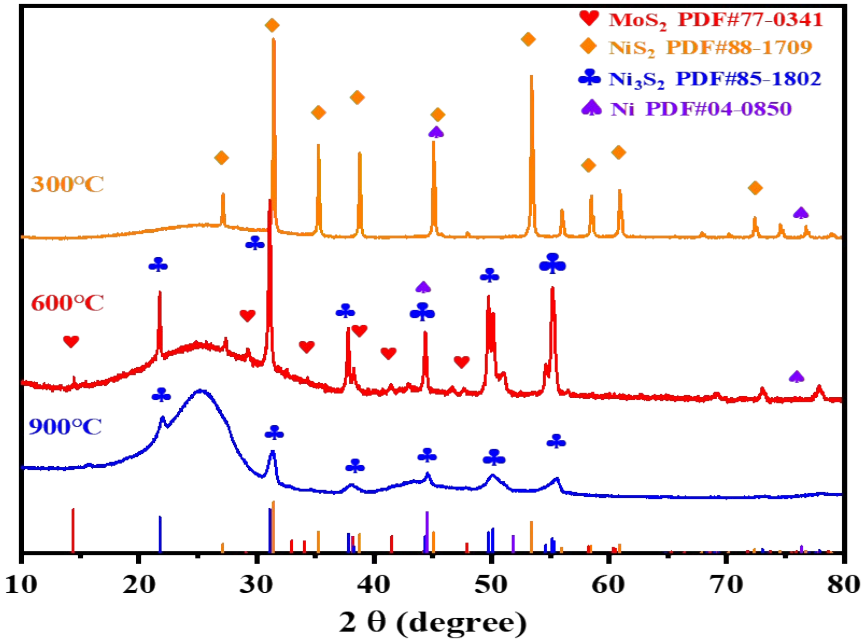


**Fig.S5.** XRD of NiMoS electrodes at different temperatures.

The morphology of NiMoS300 and NiMoS900 by the scanning electron microscope (SEM) image was recorded (**Fig. S6**). The smooth surface of NiMoS300 indicates the sulfidation is not enough (**Fig.S6A)**. However, the separated spherical ball on the surface of NiMoS900 implies the crystal of NiMo is destroyed (**Fig.S6B)**.

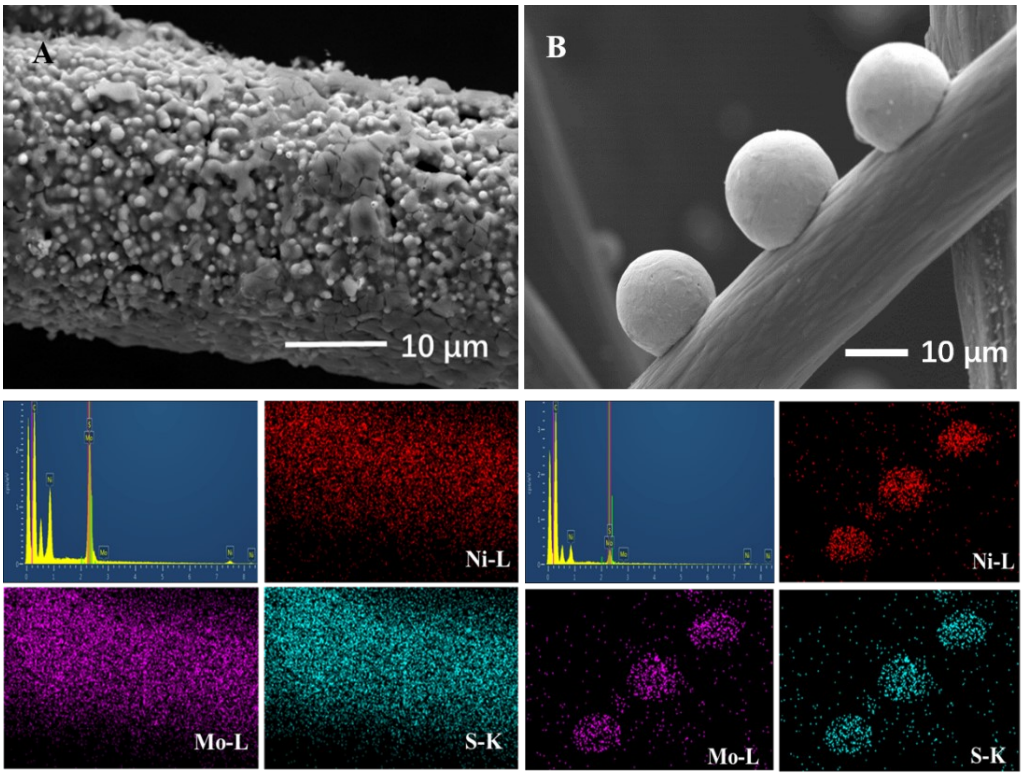


**Fig. S6.** The scanning electron microscopy image of (A) NiMoS300/CF, (B) NiMoS900/CF.

**Figure S7. CV curves of catalysts on CF (A-D) in non-faradic current region at 10-100 mV·s$^{-1}$ scan rates.**

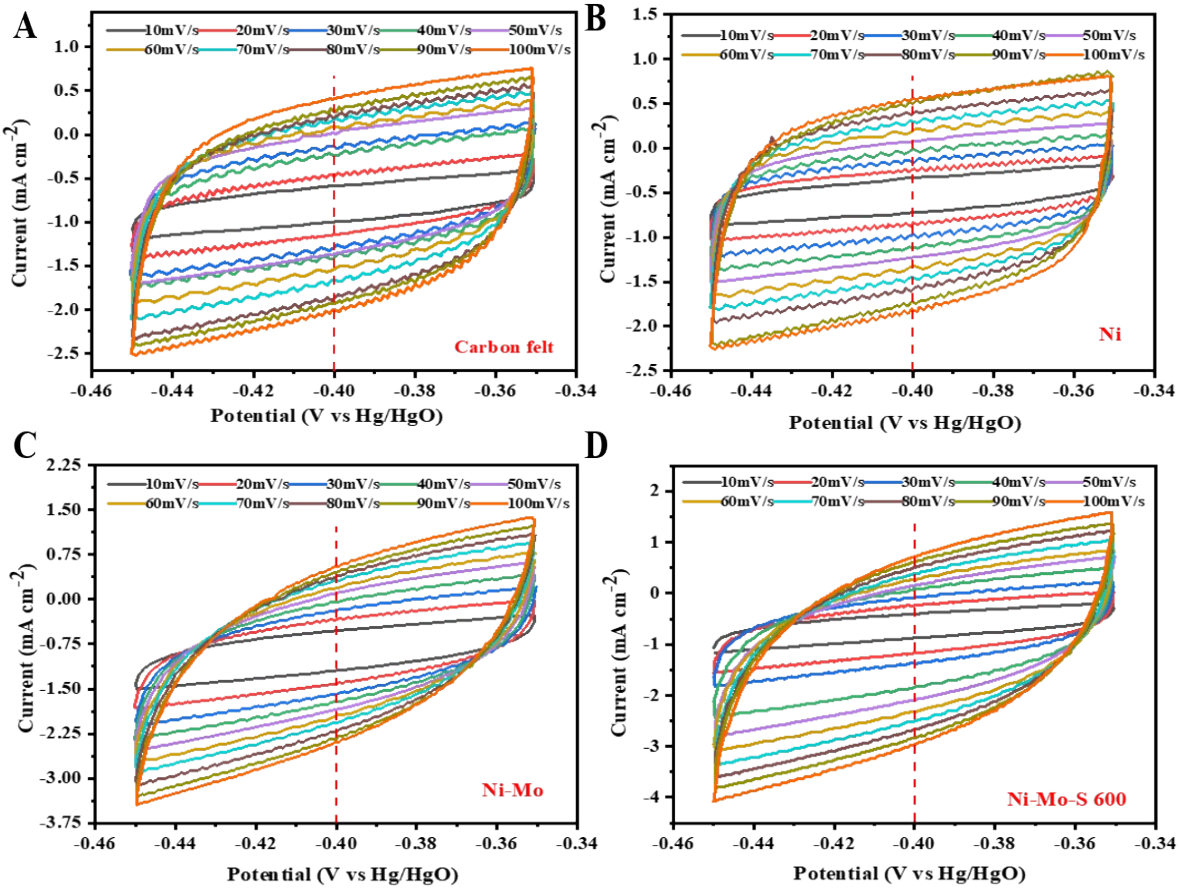

**Figure S8. Current efficiency and conversion of different electrodes for ECH of indigo under optimal conditions.**

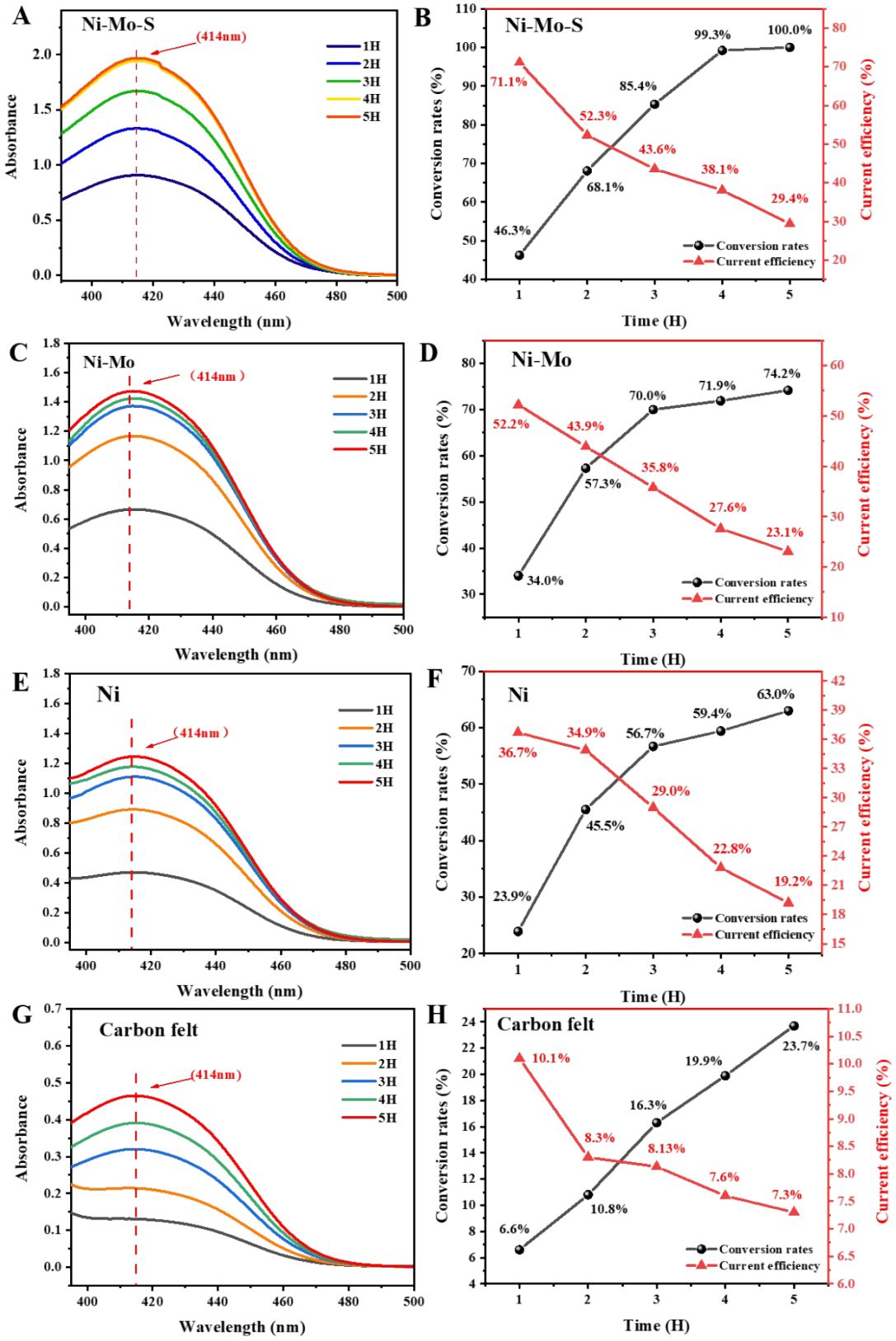

**Figure S9. Electric catalytic hydrogenation reduction of different indigo concentrations (1, 3, 5, 7g/L1) with hourly conversion rate and current efficiency**

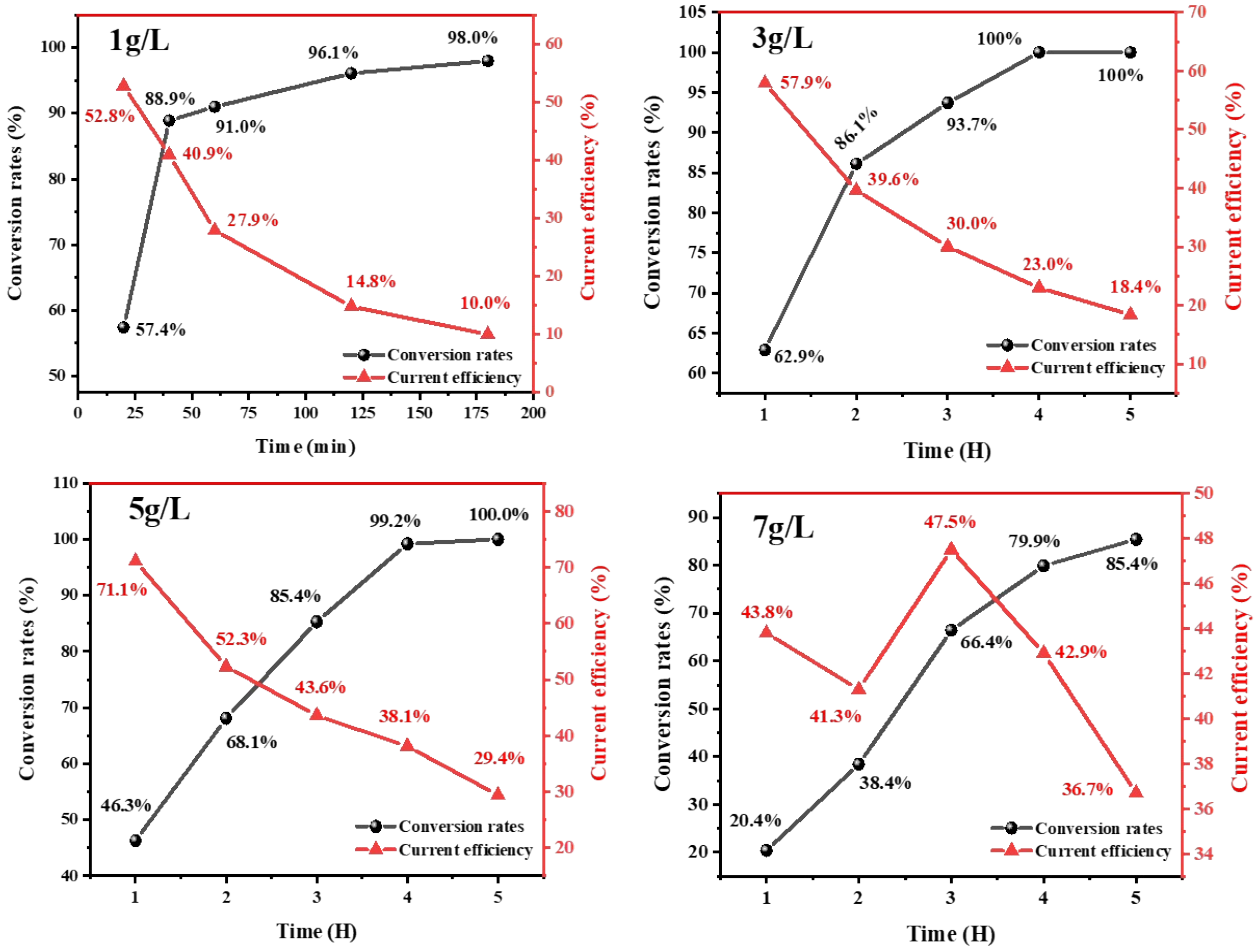

**Figure S10. The reaction device for electrocatalytic hydrogenation reduction of indigo**

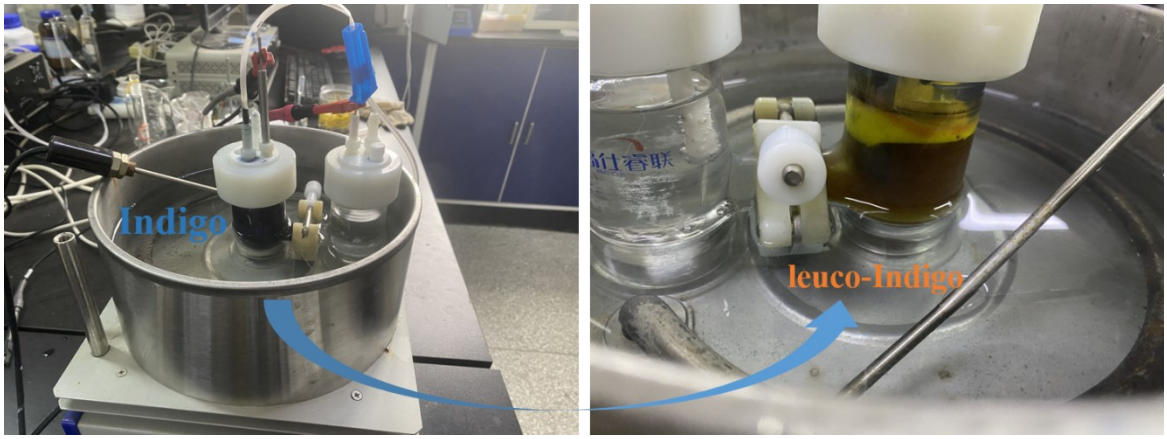

**Figure S11. Standard curves. (A) Reduced indigo fitted standard curve. (B) Indigo cryptochrome UV detection.**

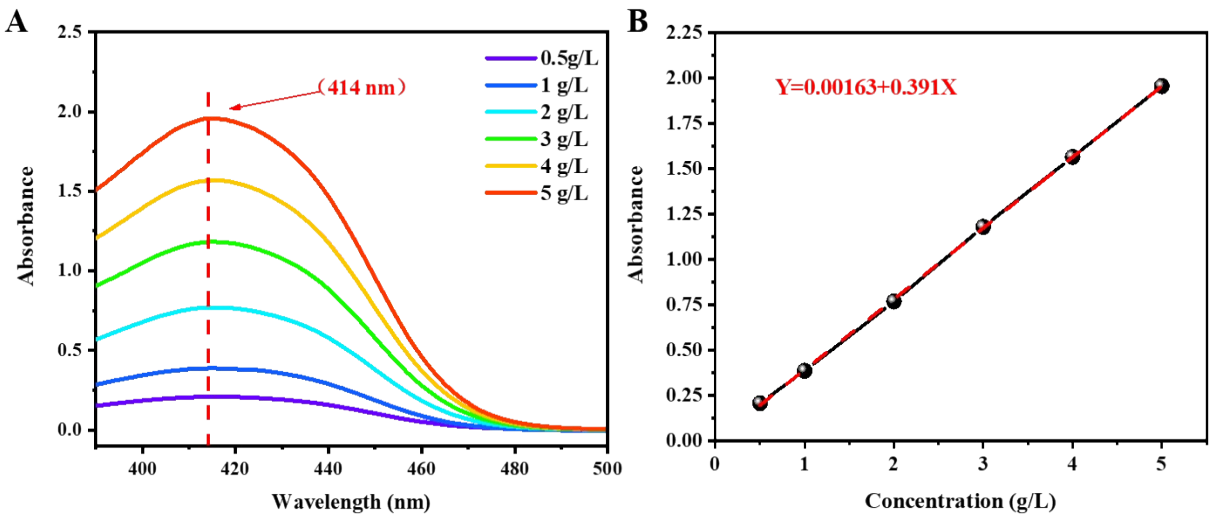

**Table S1. Compare of ECH of indigo by different electrodes.**

Conversion rate & current efficiency of ECH-reduced indigo at different electrodes under optimal conditions. System parameters: electrolyte volume 30ml，1M KOH,70℃，10 mA/cm$^2$,5g/L indigo, time 4H.

| Electrodes | Area (cm$^2$) | Conversion rate (%) | Current efficiency (%) | Reference |
|---|---|---|---|---|
| **NiMoS/CF** | **2** | **99.3** | **38.1** | **This work** |
| **NiMo/CF** | **2** | **71.9** | **27.6** | **This work** |
| **Ni/CF** | **2** | **59.4** | **22.8** | **This work** |
| **Carbon felt** | **2** | **19.9** | **7.6** | **This work** |
| **Raney Ni** | **10** | **47.5** | **3.8** | [2] |
| **NiMoP/CF** | **2** | **26.2** | **10.7** | [3] |

## References

[1] Ma Q, Hu C, Liu K, Hung SF, Ou D, Chen HM, et al., Identifying the Electrocatalytic Sites of Nickel Disulfide in Alkaline Hydrogen Evolution Reaction,J. Nano Energy.(2017)148-153.

[2] Roessler A, Dossenbach O, Marte W, Rys P, Electrocatalytic hydrogenation of vat dyes,J. Dyes & Pigments.54(2)(2002)141-146.

[3] Wei D, Liu Z, Peng J, Lü S, Jiang H, Yang F, et al., Electrodeposited NiMoP catalysts on carbon felt for hydrogenation of indigo during electrocatalytically splitting water,J. International Journal of Hydrogen Energy.47(64)(2022)27566-27578.http://doi.org/10.1016/j.ijhydene.2022.06.101